Intelligent MPPT Control of Stationary and Dual-axis Tracking Grid-connected Photovoltaic System

Layachi Zaghba, Messaouda Khennane, Abdelhalim Borni, Amor Fezzani, Idriss Hadj Mahammed and Abdelhak Bouchakour
Applied Renewable Energy Research Unit, URAER, Renewable Energy Development Center, CDER, 47133, Ghardaïa, Algeria

Keywords: Neural Network, Boost Converter, MPPT Control, Grid-connected Photovoltaic System, Dual-axis Tracking, Fixed Array.

Abstract: This paper study a performance comparison between 6 kWp dual-axis tracking system and an identical fixed inclination system on a sunny day (City of Ghardaia in South of Algeria) based on the MPPT approach of artificial neural networks. The first goal of this work is to extract the maximum power point of the photovoltaic group. The second objective, a comparison between dual-axis tracking system and an identical fixed inclination system is conducted. Simulation is carried out in Matlab/Simulink and the results show the excellent performance, high efficiency, low error, very short response of the neural network approach compared to a classical method (P&O). Results are reported to show also the effectiveness of the tracking system of about 25% in energy efficiency, therefore is confirming the economic importance of this type of system.

1 INTRODUCTION

In literature, several research works focused on various MPPT control techniques. These commands are selected based on their needs (complexity, cost, precision, convergence speed). Hill climbing, perturbs and observe (P&O) and incremental conductance are the three most popular methods, because they have the advantage of easy implementation. It is based on the disruption of the system with a constant voltage/duty cycle, and checks its behavior (Ouchen, 2016; Borni,2017). In recent years, intelligent controller techniques were used for the MPPT such as neural network to overcome these drawbacks (Ouchen, 2016; Borni, 2017).

In this paper, the first part, neural network and P&O MPPT controllers are applied to control a dual-axis tracking system and an identical fixed inclination system. The second part, we present the results of two-axis tracking and without tracking (fixed system). In addition a comparison will be presented the economic utility and the importance of the dual axis tracking system in terms of generated power.

2 GLOBAL IRRADIATIONS ON INCLINED SURFACES

Liu Jordan model based on mathematical equation was used in order to calculate different components of solar radiation (Zaghba, 2015; Astudillo, 2015; Kebour, 2017).

2.1 Direct Solar Radiation

The direct solar radiation estimated on inclined surface without being diffused by the atmosphere is given by:

$$S_i = S_{oh} R_b \quad (1)$$

Where, S_{oh} and R_b are respectively the direct solar radiation measured on horizontal surface and the tilt factor:

$$S_{oh} = A\sin(h)\exp\left(\frac{-1}{C\sin(h+2)}\right) \quad (2)$$

$$R_b = \frac{\cos(\emptyset - i)\cos(\delta)\cos(\omega) + \sin(\emptyset - i)\sin(\delta)}{\cos(\emptyset)\cos(\delta)\cos(\omega) + \sin(\emptyset)\sin(\delta)} \quad (3)$$

Zaghba, L., Khennane, M., Borni, A., Fezzani, A., Mahamed, I. and Bouchakour, A.
Intelligent MPPT Control of Stationary and Dual-axis Tracking Grid-connected Photovoltaic System.
DOI: 10.5220/0009772901990205
In *Proceedings of the 1st International Conference of Computer Science and Renewable Energies (ICCSRE 2018)*, pages 199-205
ISBN: 978-989-758-431-2

δ: Declination angle, h: height of the sun, ϕ: latitude, ω: hour angle and i: tilted angle.

With:

$$\delta = 23.45 \sin\left[\frac{360}{365}(N + 284)\right] \quad (4)$$

$$\sin(h) = \cos(\delta)\cos(\emptyset)\cos(\omega) + \sin(\emptyset)\sin(\delta) \quad (5)$$

$$\omega = 15(12 - TSV) \quad (6)$$

2.2 Diffuse Solar Radiation

The equation of diffuse solar radiation given by Liu & Jordan model which takes into account the isotropic part of sky is:

$$D_i = D_{oh}\left(\frac{1+cos(i)}{2}\right) \quad (7)$$

Where, $D_{oh}$is the diffuse solar radiation measured on horizontal plane.

$$D_{oh} = B(\sin(h)^{0.4} \quad (8)$$

B is a constant which reflect the nature of the sky.

2.3 Reflected Solar Radiation

For an inclined plane, the reflected radiation can be expressed by:

$$D_{re} = \rho.(S_{oh} + D_{oh}).\left(\frac{1-\cos(i)}{2}\right) \quad (9)$$

ρ: Albedo.

The reflected solar component in a horizontal plane is zero.

2.4 Global Solar Radiation

The total solar radiation measured or estimated on an inclined plan is given by:

$$G = S_i + D_i + D_{re} \quad (10)$$

3 PHOTOVOLTAIC SYSTEM

Figure 1 shows the considered PV system, in the first stage, the output of the photovoltaic generator is connected to a boost converter on which the MPPT control strategy is applied to increases the voltage of the PV to a suitable level for the DC-AC inverter. The second stage is applied and DC-AC converter connected to a grid through à filter.

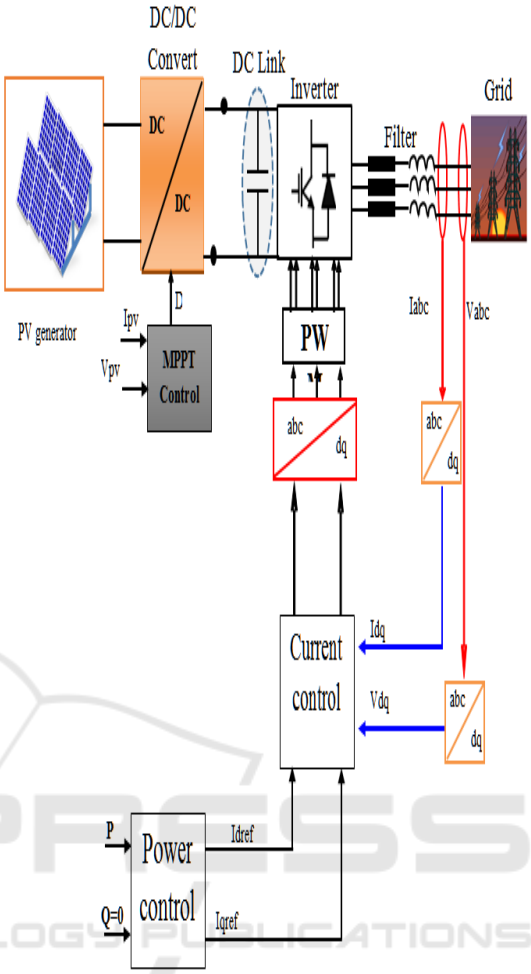

Figure 1: Grid connected PV system.

3.1 Photovoltaic Module

For this work, the 6 kWp PV generator contains 20 series modules and 5 parallel modules. Each one presents the following characteristics: Nominal peak power: 60 W, Nominal voltage: 17.1 V, Nominal current: 3.5 A.

Table 1: Electrical characteristics of 6 kwp photovoltaic arrays.

Parameter		**Value**
Maximum Power	P_{PV}	6000W
Voltage at Pmax	V_{MPP}	342 V
Current at Pmax	I_{MPP}	17.5A
Open Circuit Voltage	Voc	422V
Short Circuit Current	Isc	19 A

3.2 Boost Converter

The schematic diagram of DC-DC boost converter connected to photovoltaic generator to a resistive load is shown in Figure 2.

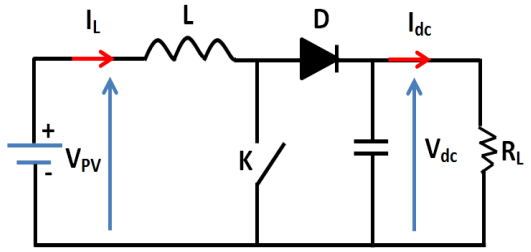

Figure 2: DC-DC Boost converter.

The state-space averaged model of the boost converter can be written as (Zaghba[1], 2017; Zaghba[2], 2017):

$$\begin{bmatrix} \dot{I}_L \\ \dot{V}_{dc} \end{bmatrix} = \begin{bmatrix} 0 & -\frac{1}{L}(1-u) \\ \frac{1}{C}(1-u) & -\frac{1}{C.R_L} \end{bmatrix} \begin{bmatrix} I_L \\ V_{dc} \end{bmatrix} + \begin{bmatrix} \frac{1}{L} \\ 0 \end{bmatrix} \quad (11)$$

Where u is the duty cycle, V_{pv} is the input voltage to the boost converter, I_L is the inductor current, C is the capacitance, R_L is the load resistance and V_{dc} is the DC link output. The equation (11) can be written as:

$$\begin{cases} \dot{x_1} = -\frac{1-u}{L}x_2 + \frac{1}{L}u \\ \dot{x_2} = \frac{1-u}{C}x_1 + \frac{1}{RC}x_2 \end{cases} \quad \text{Where } x = [I_L, V_c] \quad (12)$$

3.3 P&O MPPT Method

Figure 3 shows the flowchart of the P&O method, current and voltage are required to determine the power of the PV at each moment where the evolution of power is calculated and analyzed after each voltage disturbance (Ouchen, 2016; Borni, 2017).

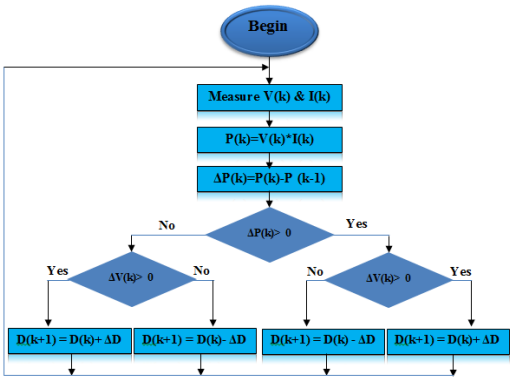

Figure 3: Flowchart of Perturb and observe MPPT.

3.4 Artificial Neural Network MPPT

The ANN is used as an intelligent control MPPT approach of the Boost converter; the simpler architecture contains three layers as shown in Fig. 4. The input layer receives the extern data (temperature and irradiation). The second layer, hidden layer, contains several hidden neurons which receive data from the input layer and send them to the third layer, output layer (output voltage).

The relationship between the inputs and output formulated as (Mellit, 2013):

$$y = \sum_{i=1}^{k} W_i \varphi(x) + w_0 \quad (13)$$

Where x: Neural inputs, Wi: Neuronal network weights, y: the output of the system.

The training of the network was provided by back propagation process using the Levenberg-Marquardt algorithm. After the learning of the network we have taken the adjusted weights and we used them with feed-forward equations into a Simulink file "embedded function" to control the PV system with the values of D provided automatically.

Back propagation algorithm used to update the weights and biases and to minimize a mean squared-error performance index given as (Mellit, 2013):

$$J = \frac{1}{2}\sum_{i=1}^{N}\left(y_i^{des} - y_i\right)^2 \quad (14)$$

Where: y_i^{des} the i- th desired output of the system. The update of Wi is done according to the following rule (Mellit, 2013):

$$w_{ij}^{k}(t+1) = w_{ij}^{k}(t) - \Delta w \quad (15)$$

We build a very rich database, which has a lot of information that will be used to learn and test the neural network on different levels of irradiation and temperature. For this phase, the following table has been realized:

Table 1: RNA training table.

T(C°) G (W/m²)	10	15	25	40	55	70
200	310.8	308.3	305	292.7	292.3	277.8
300	323.2	319.5	314.5	304.7	306.1	287.6
400	327.9	327.2	321.7	314.5	314.8	299.6
500	336.2	333.3	327.5	321	320.6	306.1
600	340.6	336.9	333.3	326.4	326.1	310.8
700	343.9	340.6	335.9	330.8	329.3	315.5
800	347.1	345.3	339.5	333.7	333.7	319.9
900	349.7	347.8	342.8	336.2	336.6	323.2
1000	352.6	350.4	350	339.9	339.5	326.4

The following Matlab code creates a feed-forward neural network:

```
P= [Temperature Data; Irradiation Data];
T= [Optimal voltage data];
net=newff(minmax(P),[40,3,1],
{'tansig','tansig','purelin'},'traingd');
net.trainParam.epochs=1000;
net.trainParam.goal=1e-3;
net.trainParam.show=50 ;
net.trainParam.lr=0.05;
[net,tr]=train(net,P,T);
a=sim(net,P)
gensim(net)
```

The conception of the MPPT control proposed shown in Fig.3.

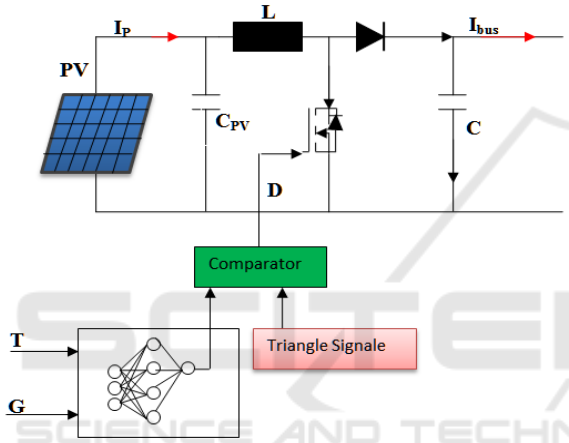

Figure 4: Topology of the ANN network for MPPT control.

3.5 Grid Side Power Control

The objective of the inverter control is to synchronize the phase's frequency between the grid and the PV, and to regulate the DC link voltage to a constant value. Fig.1 shows the connection between the inverter and the grid.

The voltage of three-phase power grid given by the following equations (Boudaraia, 2016):

$$\begin{cases} e_x = E_m \cos wt \\ e_y = E_m \cos(wt - \frac{2\pi}{3}) \\ e_z = E_m \cos(wt + \frac{2\pi}{3}) \end{cases} \quad (16)$$

E_m: The peak value of voltage in power grid, w: The angular frequency of power grid.

By applying Kirchhof's laws, we can write the voltage equation:

$$\begin{cases} e_x = L\frac{d}{dt}i_x + Ri_x + v_x \\ e_y = L\frac{d}{dt}i_y + Ri_y + v_y \\ e_z = L\frac{d}{dt}i_z + Ri_z + v_z \end{cases} \quad (17)$$

Applying Park transformation, we obtain:

$$\begin{pmatrix} \frac{di_d}{dt} \\ \frac{di_q}{dt} \end{pmatrix} = \frac{1}{L}\begin{pmatrix} -R & wL \\ wL & -R \end{pmatrix}\begin{pmatrix} i_d \\ i_q \end{pmatrix} - \frac{1}{L}\begin{pmatrix} e_d \\ e_q \end{pmatrix} + \frac{1}{L}\begin{pmatrix} v_d \\ v_q \end{pmatrix} \quad (18)$$

4 RESULTS AND DISCUSSIONS

The study was conducted in Ghardaia, Algeria located at 32.48° North and 03.67° East. This site is characterized by hot and dry climate in the summer with an average temperature of 38°C. The solar radiation on the region is very high; the horizontal solar radiation is very important, in summer, it can reach 1040 Wh/m². The wind is dry and hot with an average speed between one and 2.5 m/s (Boukhelkhala ,2016). Simulation studies have been carried out in Matlab/Simulink environment to verify the proposed artificial neural network method for a sunny day (Ghardaia site).

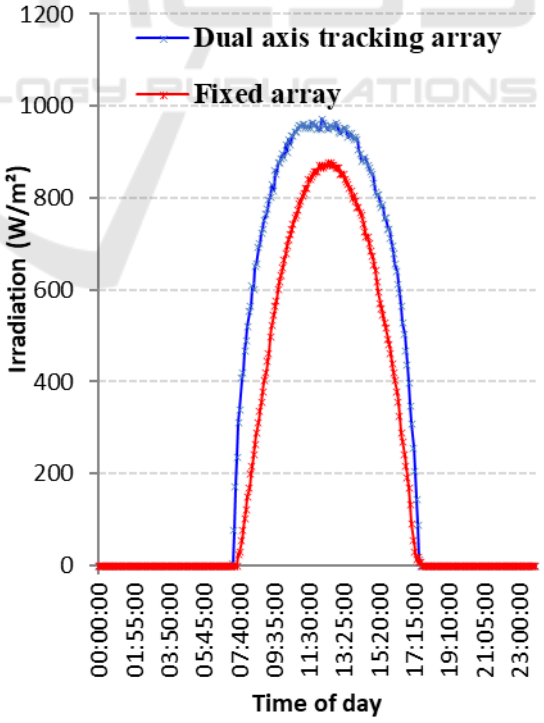

Figure 5: Variations of irradiance over time in a sunny day (Ghardaia site).

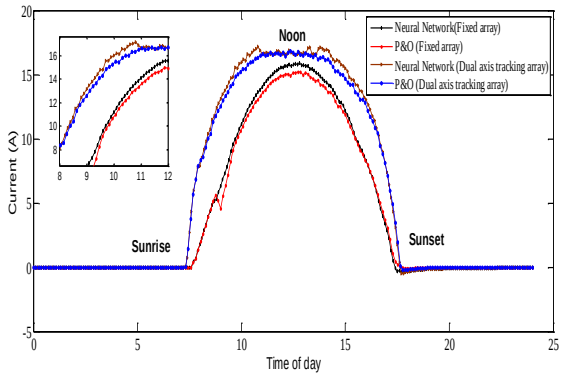

Figure 6: Output current of the PV (Fixed array and dual axis tracking array).

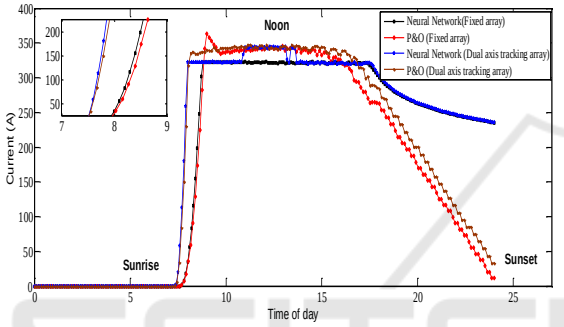

Figure 7: Output voltage of the PV in a sunny day (Fixed array and dual axis tracking array).

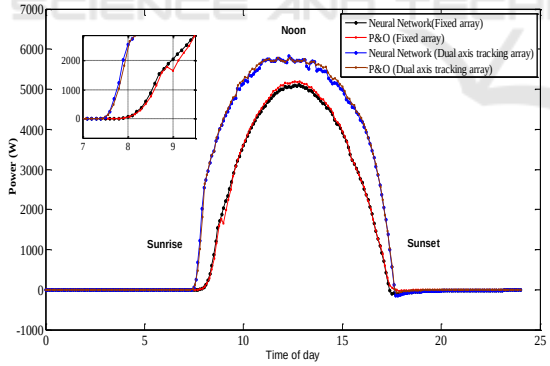

Figure 8: Output power of the PV (Fixed array and dual axis tracking array).

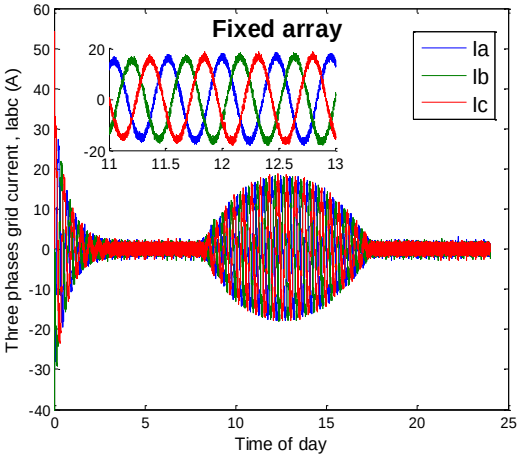

Figure 9.a: AC three phase's grid currents using P&O MPPT controller (fixed array).

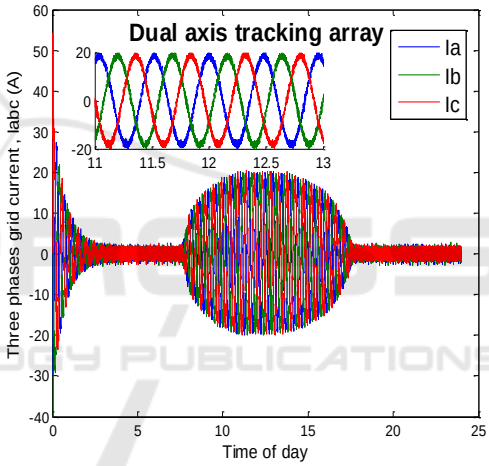

Figure 9.b: AC three phase's grid currents using P&O MPPT controller (dual axis tracking).

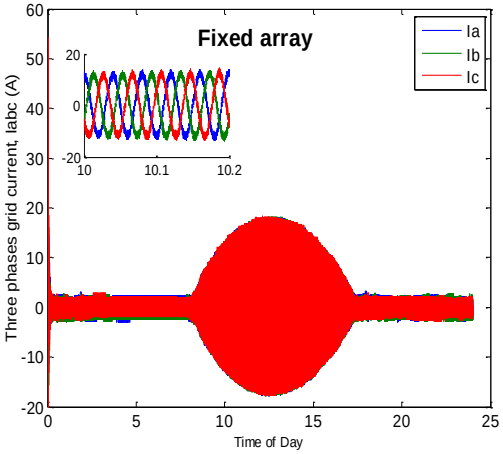

Figure 10.a: AC three phase's grid currents using neural network MPPT approach (fixed array).

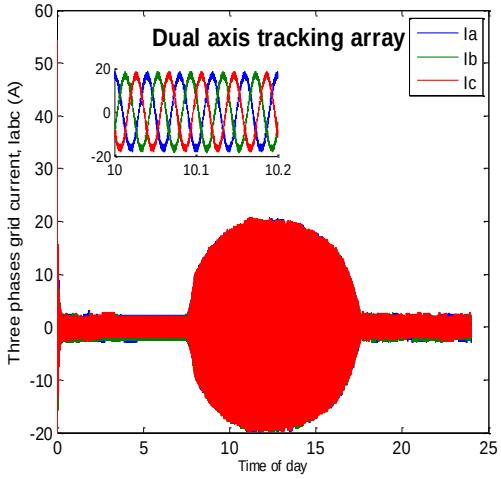

Fig. 10.b: AC three phase's grid currents using neural network MPPT approach (dual axis tracking).

Fig. 6, Fig. 7 and Fig. 8 show the waveforms of the output voltage, current, and power of the PV respectively. Here we can see that both P&O and neural network approach were successfully able to track the maximum power point for a PV panel at any given irradiation. The neural network –based MPPT algorithm can quickly and accurately find the maximum power of each type (fixed and tracking array) and the system achieved a true sense of the maximum power output. The P & O algorithm strongly depends on the initial conditions and it presents oscillations around the optimal value. This algorithm is bad behavior following a sudden change in irradiation .The results show that neural network optimization technique given better results compared to P&O. As shown, for south facing fixed surface solar power varies over the day, peaking at the solar noon where tracking system has flatter hourly energy production profile. As shown, the value of the solar energy produced by the fixed system approaches that of the two-axis system between 11 am and 14 pm, but it moves away during the hours of the sunrise and the hours of the end of the afternoon.

We can see also that the power production of a PV system is directly related to the amount of solar irradiance incident on the array. On average, tracking systems yield a higher average normalized power output under sunny conditions when compared to stationary systems since they are always oriented nearly perpendicular to direct beam radiation.

In addition, this paper demonstrates the importance and efficiency of dual tracking system. The results indicate that the solar tracking system generated more energy about 25% compared to the power generated by identical fixed solar panels.

5 CONCLUSIONS

The neural network based MPPT control has clearly demonstrated its utility and the effectiveness in tracking the maximum power point of two identical photovoltaic systems, the first is equipped with a solar tracker while the second is without a tracker and shows an excellent performance, high efficiency, low error, very short response time, high dynamics for both inverter and MPPT compared to classical MPPT control.

ACKNOWLEDGMENT

This project was financially supported by the Directorate General for Scientific Research and Technological Development - Algerian Ministry of Higher Education and Scientific Research.

REFERENCES

Ouchen, S., Abdeddaim, S., Betka, A., Menadi, A., Experimental validation of sliding mode-predictive direct power control of a grid connected photovoltaic system, feeding a nonlinear load, Solar Energy 137 (2016) 328–336.

Borni, A., Bouarroudj, N., Bouchakour, A. and Zaghba, L., P&O-PI and fuzzy-PI MPPT Controllers and their time domain optimization using PSO and GA for grid-connected photovoltaic system: a comparative study ,Int. J. Power Electronics, Vol. 8, No. 4, 2017.

Zaghba, L., Terki, N., Borni, A., Bouchakour, A., Benbitour Née Khennane Messaouda, Adaptive intelligent MPPT controller comparison of Photovoltaic system under different weather Conditions of ghardaia site (south of Algeria), Journal of Electrical Engineering, Volume 15 / 2015 - Edition: 3.

Astudillo, D. P., Bachour, D., 2015. Variability of measured global horizontal irradiation throughout Qatar. Sol. Energy 119, 169–178.

Kebour, O., Arab, A. H., Abdelkader Hamid, Kamel Abdeladim, Contribution to the analysis of a stand-alone photovoltaic system in a desert environment, Solar Energy 151 (2017) 68–81.

Zaghba[1], L., Khennane, M., Terki, N., Borni, A., Bouchakour A., Fezzani, A., Hadj Mahamed, I., and Oudjana, S. H., The effect of seasonal variation on the performances of grid connected photovoltaic system in southern of Algeria, AIP Conference Proceedings,

1814, 020005 (2017); https://doi.org/10.1063/1.4976224.

Zaghba[2], L., Borni, A., Khennane, M., Terki, N., Fezzani, A., Bouchakour, A., Hadj Mahamed, I., Oudjana S. H., Experimental typical meteorological years to study energy performance of a PV grid-connected system, Energy procedia, Volume 119, July 2017, Pages 297-307.

Mellit, A., Sa_glam, S., Kalogirou, S. A., Artificial neural network-based model for estimating the produced power of a photovoltaic module, Renewable Energy, 60 (2013) 71e78.

Boudaraia, K.; Mahmoudi, H.; El Azzaoui, M., Modeling and Control of Three Phases Grid Connected Photovoltaic System, Renewable and Sustainable Energy Conference (IRSEC), 2016 International, DOI: 10.1109/IRSEC.2016.7984004.

Boukhelkhala, I., Bourbiab, F., Thermal Comfort Conditions in Outdoor Urban Spaces: Hot Dry Climate -Ghardaia- Algeria, Procedia Engineering, 169 (2016) 207 – 215.